ACS APPLIED MATERIALS & INTERFACES

Research Article

www.acsami.org

Revealing Strong Nanocomposite Hydrogels Reinforced by Cellulose Nanocrystals: Insight into Morphologies and Interactions

Jun Yang,*[,†] Jing-Jing Zhao,[‡] Feng Xu,[†] and Run-Cang Sun[†]

[†]College of Materials Science and Technology, Beijing Forestry University, Beijing 100083, China

[‡]Beijing SL Pharmaceutical Co., LTD, Beijing 100049, China

Supporting Information

ABSTRACT: Understanding the reinforcement mechanism by dispersing nanoscale particles into a polymer matrix is a critical challenge toward refining control of the composite properties. In this paper, the morphologies and interactions of cellulose nanocrystal/poly(acrylic acid) (CNC/PAA) nanocomposite hydrogels are demystified based on a facile synthetic platform. Two sources of CNCs with different aspect ratios are applied to model the reinforcement process, and the uniaxial tensile measurements indicate that the CNC aspect ratio and the nanocomposite mechanical behaviors are coupled, where the values of aspect ratios and nonpermanent interactions between the fillers and matrix dominate the reinforcement. Dynamic mechanical analysis is performed to examine the nature of the constrained polymer as the semicrystalline fractions, and the results indicate that polymer chain mobility in the vicinity of CNC surfaces is significantly reduced, providing new insight into the origin of the reinforcement mechanism. Rheological analysis and transmission electron microscopy observations show that both stepwise dissociation and polymer chain rearrangements contribute to the viscoelastic behaviors of the nanocomposite hydrogels. The increased modulus of the hydrogels is correlated to the volume of the constrained polymer, where the CNCs impart significant enhancement to the entanglement network. This study of the structure−property relationship deepens the understanding of the filler reinforcement mechanism and provides valuable knowledge for designing high performance nanocomposite hydrogels from cellulose as a raw material.

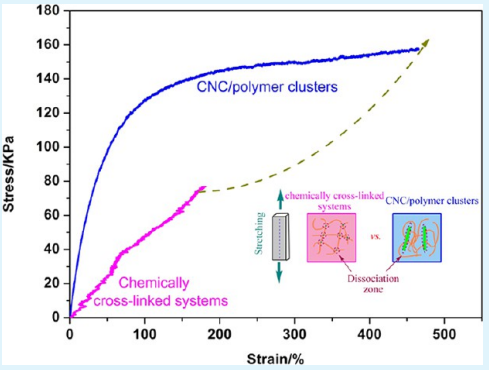

KEYWORDS: *nanocomposite, hydrogel, cellulose, morphology, interaction*

1. INTRODUCTION

The last decade has witnessed the rapid development and investigation of polymer nanocomposites, because of their unique optical, mechanical, and electronic properties at a low loading of nanoscale fillers, as compared to their bulk counterparts.[1−4] Inspired by the toughening mechanism of carbon black filled rubbery, the incorporation of mechanically robust, high aspect ratio nanoscale fillers into a polymer matrix is of great interest for researchers from academia to industry.[5−8] Cellulose is the most abundant organic resource and has applications in various areas as diverse as composite materials, drug delivery, textiles, and personal care products.[9]The application of lignocellulosic biomass as a reinforcing filler in composites has superior environmental and biological compatibility as compared to other leading candidates, such as clay, carbon nanotubes, and silicate.[10] Moreover, because of benefits from advances in polymer synthesis, some unique routes are now available for the preparation of functional cellulose-based composites.[11]

Hydrogels are a spectacular form of soft matter with water-swollen, cross-linked polymeric structures that respond to external perturbations.[12−14] According to the type of cross-links present in a network, polymeric hydrogels are commonly classified as "chemical" or "physical" hydrogels.[15]Chemically cross-linked hydrogels consist of polymer chains that are interconnected by permanent covalent bonds, which often make them brittle.[14] In sharp contrast, physical hydrogels, dynamic in nature, are defined as materials whose chains are bridged via reversible noncovalent connections.[15] Physical cross-linking originates from either entanglements between dynamic colloidal species or noncovalent nanoparticle interactions between polymer chains. These small colloidal nanoparticles interpenetrate into large units, where entanglement subsequently leads to the secondary structure and properties that are not present in the primary constituents.[2] Due to the presence of solvent (normally water) during the gel formation process, hydrogels are always soft and fragile, and high strength becomes one of the most remarkable properties.[14,16,17] It has been known that the poor mechanical performance of most synthetic hydrogels mainly stems from the low resistance to crack propagation and lack of an efficient energy dissipation mechanism in the network.[18] Therefore, to obtain a tough and stretchable gel, from the reinforcing mechanism of nanocomposite hydrogels, one has to increase

Received: August 29, 2013
Accepted: December 2, 2013
Published: December 2, 2013

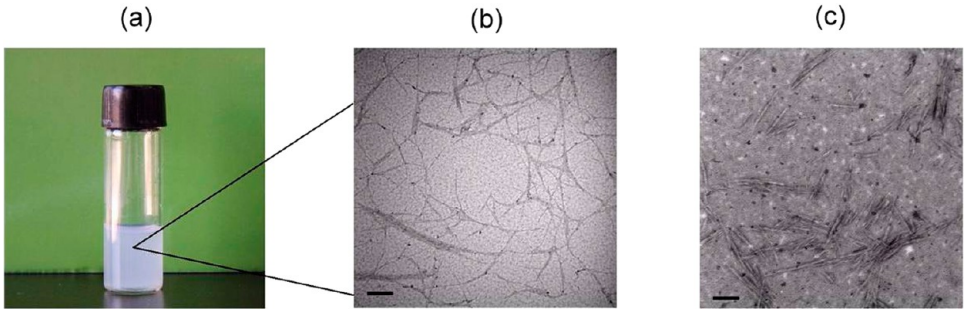

Figure 1. Pictures of CNCs. (a) Photograph of CNC aqueous solution (2 mg/mL). (b) TEM images of CNCs prepared from microcrystalline cellulose and (c) pulp fiber. (bar = 100 nm).

the sacrificial bonds that effectively dissipate energy during deformation, instead of permanent cross-links.[19,20] Over the past few years, several reinforcement strategies, including the design of heterogeneous double network by Gong,[21] development of ideal network structure by Okumura,[22] and the combination of organic and inorganic components in hybrid hydrogels by Haraguchi,[23] have been advanced to overcome the mechanical weakness.

Several hypotheses have been proposed to rationalize the reinforcement of polymeric materials by incorporation of rigid particles.[24,25] Moreover, increasing reports validate a scenario that the interactions between the matrix and fillers may be more important for property enhancement even at a low filler loading.[26,27] Inspired by the nanoscale interactions in natural composites, a synthetic polymer composite containing attractive interactions between the fillers and polymer matrix is developed to (1) explore the role of interfacial layer on the mechanical reinforcement, and (2) polymer chains can wrap around neighboring fillers and form a "bridge network" where the particles act as physical cross-links.[25] With this aim in mind, we prepare strong nanocomposite hydrogels by attractive interactions between cellulose nanocrystals (CNCs) as fillers and poly(acrylic acid) (PAA) as the matrix and interpret the reinforcement mechanism via reversible network arrangement. The hydrogel network microstructure changes under stress are characterized by cryo-transmission electron microscopy (cryo-TEM). According to rheological analysis, the mechanical enhancement significantly relates to the volume of the constrained polymer chains around the CNC surface. Overall, the results obtained here are expected to demystify the relationship between the microscopic structure and macroscopic function and thus shed some light on the fast ongoing field of tough nanocomposite hydrogels.

2. EXPERIMENTAL SECTION

Materials. Two sources of cellulose, including commercial microcrystalline cellulose (MCC) received from Sinopharm Chemical Reagent Co. and pulp fiber obtained from Donghua Pulp Factory, were applied to prepare cellulose nanocrystal (CNC) suspensions by sulfuric acid hydrolysis according to the method proposed by Dufresne et al. with minor modification.[28] In brief, about 4 g of cellulose was added to 200 mL of 55 wt % sulfuric acid at 50 °C for 2 h under mechanical stirring (200 rpm). The suspension was diluted with deionized water and concentrated by centrifugation, followed by dialysis against water until neutrality. The suspension (2 mg/mL) was further dispersed by ultrasonic treatment to produce a homogeneous colloidal solution. The organosilane γ−methacryloxypropyl trimethoxy silane (Sigma), where siloxane bonds were formed through the reaction between hydroxyl groups on CNC surface and silanols, and at the other end of the silane bridge can create covalent bonds with polymer matrix (Figure S1, Supporting Information),[29,30] was used to modify the CNCs before the in situ graft. All other reagents were of analytical grade and used without further purification.

Synthesis of Nanocomposite Hydrogels. To a 50 mL beaker were added deionized water (20 g), acrylic acid (AA, 4 g), potassium persulfate (10 mg), and CNCs. The sample codes for nanocomposite gels (x% CNC gels) were defined by the weight concentration of the CNC against water (constant at 20 g). For example, 0.2% CNC gel referred to a gel loaded with 40 mg CNC. The precursor solutions were sonicated and stirred vigorously to ensure good dispersion and degassed under vacuum. Then the resultant solutions were poured into PTFE molds under nitrogen atmosphere at 65 °C for 4 h. For neat chemically cross-linked hydrogels, they were prepared by the same procedures except an organic cross-link *N,N′*-methylenebisacrylamide (BIS, y% against AA weight) was used instead of CNC. The resulting nanocomposite hydrogels were peeled from the mold and immersed in distilled water for 72 h to remove unreacted monomer and unlinked polymers. For tensile measurements and rheological measurements, the rectangular strips with dimensions of 2 mm in height × 40 mm in length × 8 mm in width and cylindrical-shaped samples with dimensions of 25 mm in diameter × 1 mm in height were prepared, respectively.

Characterizations. *Tensile Testing.* The mechanical properties of the hydrogels were measured using a Universal Material Testing machine from Zwick Z005 (Ulm, Germany) at room temperature. Both ends of the sample were clamped and stretched at a constant rate of 30 mm/min, and the specific testing method was preset by testXpert II software. A piece of sanded paper was added to the clamps to avoid slipping of the wet hydrogels on the alumina surface. Raw data were recorded as force versus displacement, and they were converted to stress versus strain with respect to the initial sample dimensions (2 × 8 mm^2). The fracture stress (σ) was determined from the stress−strain curves at the breaking points. For each sample, three strips were tested. The tensile hysteresis was analyzed under the same conditions in which the sample was initially stretched to a predefined strain and immediately unloaded at the same velocity.

Transmission Electron Microscopy (TEM). The morphologies of the CNCs were observed under a transmission electron microscope (JEM-1010, JEOL) using an acceleration voltage of 80 kV. Three microliters of a CNC suspension solution were deposited on a carbon-coated copper grid for 1 min before the excess was removed by a filter paper. The grid was then poststained with a 2 wt % uranyl acetate aqueous solution for the purpose of enhancing the contrast. Additional TEM experiments using cryo-TEM were performed on stretched nanocomposite hydrogels. The hydrogels were stretched uniaxially using Zwick Z005 under different strains and "fixed" with binder clips to maintain their elongated state. The stretched samples were then cryo-fractured by immersing into liquid nitrogen. Ultrathin sections (~100 nm) were cut using a Leica cold knife at −80 °C. The sections were collected on carbon grids and transferred to a cryoholder (D626, Gatan, Inc.) without any further modification, and then the vitrified sample was observed and imaged using a JEOL-2010 microscope at −140°C.

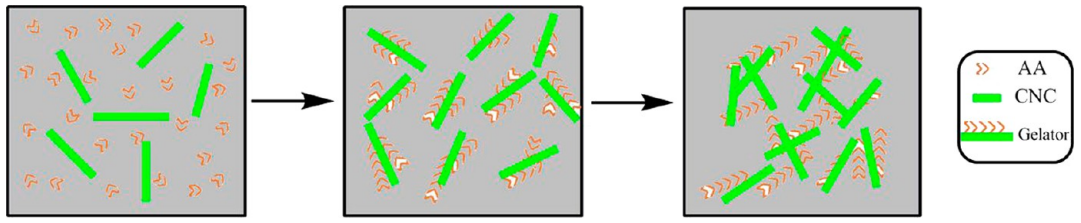

Figure 2. Schematic representation of CNC/polymer gelation, where gelators are formed by bundles of polymer coated fibers (not to scale).

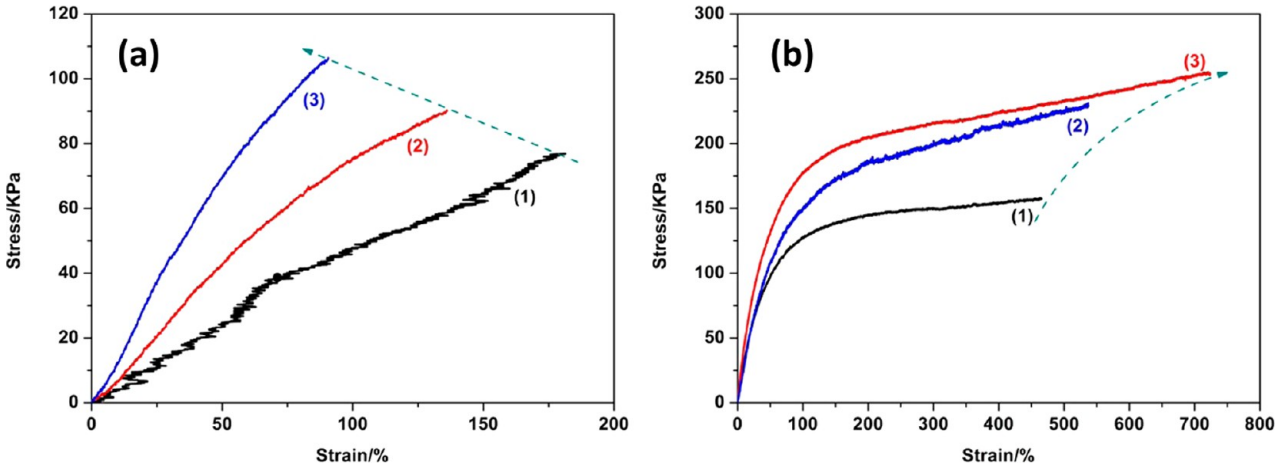

Figure 3. Tensile properties of PAA hydrogels. (a) Chemically cross-linked hydrogels prepared with BIS concentrations at (1) 1 wt %, (2) 1.4 wt %, and (3) 1.8 wt %. (b) Nanocomposite hydrogels prepared with different CNC aspect ratios (1) L/d = 14, (2) L/d = 22, and (3) L/d = 31 at a given concentration of 0.5 wt %.

Rheological Experiments. Dynamic oscillatory measurements were performed at 25 °C by shearing the gel between the parallel plates in a TA AR2000 rheometer equipped with a Peltier device for temperature control. The gels were deformed at a stress within the linear viscoelastic region by varying the frequency from 0.1 to 100 Hz at a strain of 0.01 to quantify the viscoelasticity of hydrogels. For nonlinear rheological analysis, a strain induced softening phenomenon was examined in the range of 0.01 to 10% at a frequency of 10 Hz.

3. RESULTS

Morphology of CNCs. In this study, two sources of cellulose, including commercial microcrystalline cellulose (MCC) and pulp fiber, were used to prepare CNC suspensions via sulfuric acid hydrolysis in a comparative manner. The resulting aqueous solution remained in a homogeneous colloidal dispersion to the eye without settlement for weeks (Figure 1a). This phenomenon is ascribed to the presence of the electrostatic repulsion between the negatively charged sulfate ester groups on their surface, which are a byproduct of the sulfuric acid hydrolysis.[6] In fact, this electrostatic repulsion between CNCs promotes the formation of CNC/polymer cluster nanocomposites with homogeneously dispersed architectures. Figure1b,c shows the typical TEM images of CNCs prepared by sulfuric acid hydrolysis of MCC and pulp fiber, respectively. The rodlike CNCs derived from MCC have a length between 400 and 700 nm, whereas those from pulp are 100−200 nm in length. Thus, the TEM images of both cellulose sources reveal that fairly well-individualized CNCs derived from MCC exhibit a much higher aspect ratio (L/d = 31, N = 10) and a more pronounced reinforcing effect (see below) compared to pulp fiber derived CNCs that more readily form small bundles (L/d = 14, N = 10). As for the local aggregates in images (Figure 1c), it may be partially ascribed to the fact that negative staining is known to induce an aggregation of nanoparticles on the supporting carbon film (Figure S2, Supporting Information).[27,31]

The most challenging aspect in nanocomposite materials has been to achieve uniformly dispersed fillers in a matrix and a filler phase size of less than several hundredths of a nanometer.[1−3] By simply using an aqueous blending process, a water-soluble acrylic acid monomer could in situ graft from the surface of the CNC to generate CNC/PAA nanoparticle clusters. That is, the CNCs loaded nanocomposites are constructed from rigid CNCs and flexible PAA chains, which can be seen as bricks and mortar, respectively (Figure 2). The polymer mortar connects neighboring bricks to maintain the structural integrity and suppresses the mobility of the bricks. In addition, the driving forces for these cluster aggregations belongs to attractive interactions, where the polymer chains act as inert matrices to further enhance the structural stability by forming bulky nanocomposites from the unitary CNC/PAA colloidal nanoparticles.

Mechanical Properties. To evaluate the effect of aspect ratio of CNC on nanocomposite hydrogels mechanical reinforcement, the uniaxial tensile measurements were performed. For covalently cross-linked PAA hydrogels, one can note that they showed weak and brittle properties (Figure 3a). The increase of BIS concentration leads to the higher elastic modulus and lower fracture energy, which is similar to most irreversible covalent bond-linked polymeric materials.[15] In fact, it is even impossible to conduct tensile tests at a BIS concentration higher than 2.2 wt %, because the sample is too brittle to handle. In contrast, the nanocomposite hydrogels exhibited a much higher fracture strength and elastic modulus even at a CNC concentration as low as 0.2 wt % (Figure 3b). Furthermore, it is shown that the aspect ratio of CNC plays a

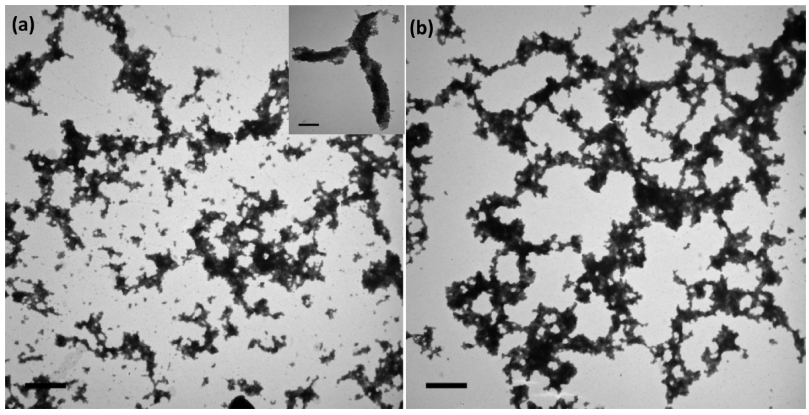

Figure 4. Cryo-TEM pictures of (a) 0.2 % CNC and (b) 0.5% CNC hydrogels (bar = 200 nm). The 0.2% CNC hydrogel has a more open and thin wall of network structure, whereas the 0.5% CNC hydrogel shows a denser network with thicker wall and smaller pores. The light gray parts between the rodlike aggregates correspond to PAA bridges and form core−shell structure (inset in panel a, bar = 20 nm).

critical role in the reinforcement behaviors. In particular, the fracture strength of the gels increased from 157 to 229 kPa as the aspect ratio of CNC increased from 14 to 22, and then the strength further increased to 254 kPa at an aspect ratio of 31. Stress, in a fiber composite, is known to transfer across fiber ends by a process known as shear-lag, suggesting the aspect ratio of filler is an important effect to lend itself to composite reinforcement.[27,32] In fact, the reasons that the wide application of CNC in nanocomposites not only stem from the CNCs high elastic moduli in both axial and transverse direction but also originate from the CNC percolation effect.[33−35] This theory reveals that the CNCs homogeneously distribute throughout the matrix without segregation and form a two-phase "molecular composite" that bound by hydrogen bonds.[33]

Stretched Hydrogels Network. To interpret network structure−property relationships (to rule out the influence of aspect ratio, the pulp fiber derived CNCs are used in the following discussion), the microscopic observation of CNC/PAA nanocomposite hydrogels under different stretched levels was performed, and the representative TEM images of network before mechanical deformation (relaxed) are shown in Figure 4. Within the examined length scale, no obvious aggregates were found, indicating well-dispersed CNC/PAA clusters within the network. According to the structures of the "relaxed" state, 0.2% CNC gels and 0.5% CNC gels show some differences in network structure (e.g., pore size and pore wall thickness): the former possesses the thinner pore wall and less-interpenetrated pores, as compared to the latter, which has uniform, thicker, and more interconnected pores.

Furthermore, the 0.5% CNC gels were chosen to examine network deformation under stress via cryo-TEM, which allows for a better understanding of how clusters rearrange at stretched states and affect properties of the resulting gels (Figure 5). Intriguingly, there exist significant network morphological changes at different stretched levels. At the initial "relaxed" state, the CNC/PAA clusters present a highly interconnected network with a thick wall (polymer shell) on the CNC surface. Then, the networks reorganize to a parallel arrangement into crystallite strands, and the pore wall and pore size become thinner and bigger, respectively. As expected, cellulose has a high cohesive energy that is greatly enhanced by the fact that the hydroxyl groups are capable of forming extensive hydrogen bonds.[33,36] Thus, these stiff and straight cellulose fillers have a considerable tendency to rearrange to

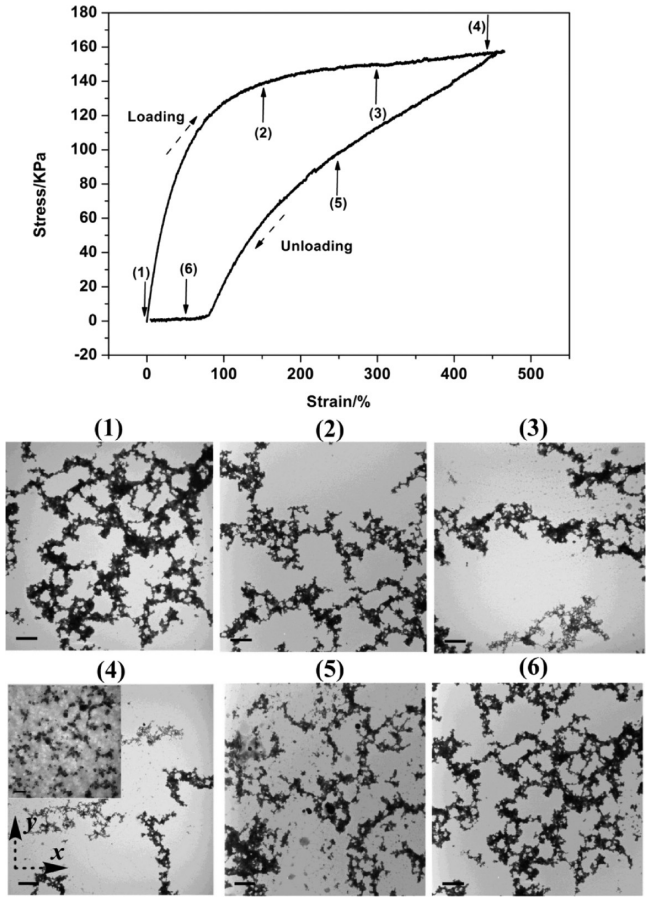

Figure 5. Cryo-TEM pictures of vitrified 0.5% nanocomposite hydrogels at different strains, which provides morphological evidence for the mobility of the CNC/PAA cluster nanoparticles (bar = 200 nm). The imaged plane is parallel to the stretching direction, where stretching direction is along the *x*-axis. The inset in panel 4 shows an enlarged stretched network under large deformations (bar = 50 nm).

their parallel conformations with stress, which is the basic moving element of the CNC/PAA fibril clusters. Besides, according to the loading−unloading cycle measurements, a major hysteresis loop is visualized here, suggesting a large energy dissipation process and absorbance of much energy to suppress the crack propagation. In fact, to be a tough hydrogel, hysteresis is critical due to it is a measure of toughness of the

materials.[37] The hysteresis of the CNC/PAA gels is related to the internal fracture of reversible interactions, which avoids the stress concentration at the crack tip and restrain crack propagation. Together with TEM observation and tensile analysis, these results indicate that the CNC/PAA clusters hierarchically rearrange the network under high strains, where the polymer chains slide at the CNC surface to withstand the large scale deformation of the hydrogel network. The recent molecular dynamic simulation also shows that the mobility of the nanofiller particle dominated the energy dissipate process,[25] suggesting the hierarchical displacement of CNC/PAA clusters is key to the performance of the nanocomposites.

Dynamic Viscoelastic Analysis. Dynamic oscillatory shear analysis was applied to study the viscoelastic behavior of the gels. In general, the magnitudes of storage moduli (G') of hydrogels varied by the type of cross-links as well as the degree of cross-link. For covalently cross-linked hydrogels, they demonstrated an almost independency of storage moduli within the observed frequency range, no matter the concentration of BIS (Figure 6a). This result indicates that the gels behave like an elastic network even at a low cross-linking level. In sharp contrast, CNC/PAA nanocomposite hydrogels showed more liquidlike behaviors and linear dependence of the storage moduli within the whole frequency window (Figure 6b). After another careful observation, the

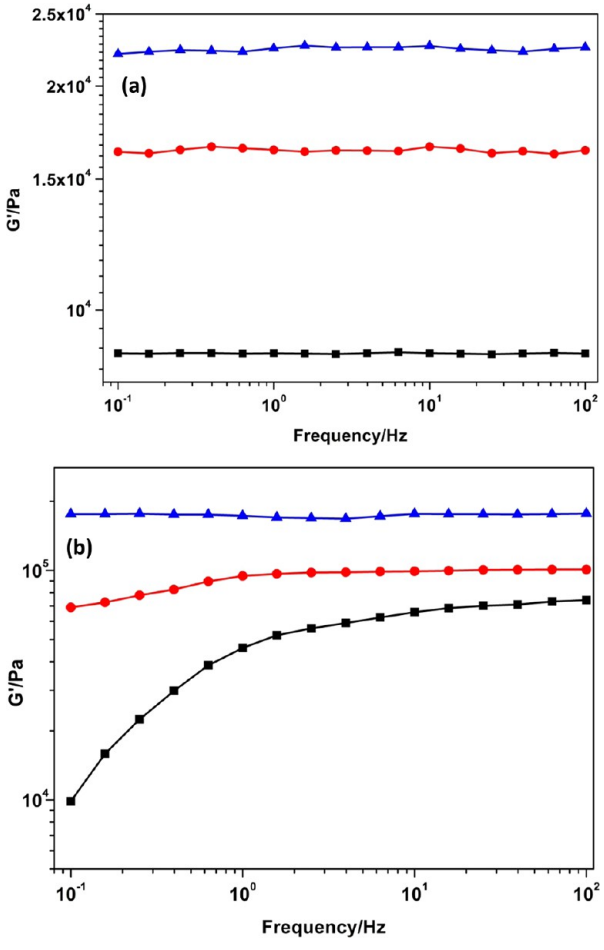

Figure 6. Evolution of storage moduli (G') as a function of frequency. (a) Chemically cross-linked PAA hydrogels at BIS concentration of 1 wt % (■), 1.4 wt % (●), 1.8 wt % (▲). (b) Nanocomposite hydrogels at CNC concentration of 0.2 wt % (■), 0.4 wt % (●), 0.5 wt % (▲).

increasing fraction of CNC reduced this dependency, and it became frequency independent at a high CNC concentration (0.5 wt %). This result is similar to the covalently cross-linked hydrogels, implying the formation of a well-developed rigid network.

A standard technique to quantify the contribution of a filler network formed by a solid phase in composite materials is a strain−sweep test on as-prepared samples.[38] The responses of hydrogels to large-amplitude oscillatory shear deformation with strain amplitudes γ increasing from 0.01% to 10% were performed (Figure 7). One can note that the storage moduli of

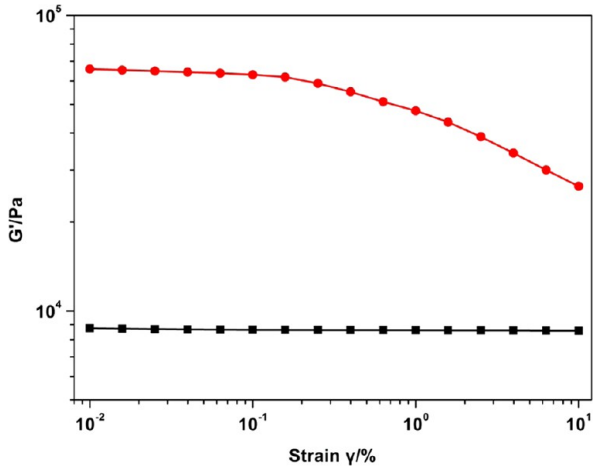

Figure 7. Storage modulus G' as a function of shear strain amplitude γ at frequency of 10 Hz. (■) Chemically cross-linked PAA at 1 wt % of BIS, (●) nanocomposite hydrogel at 0.2 wt % of CNC.

covalently cross-linked hydrogels were almost independent of strain magnitude at a given frequency. Whereas for 0.2% CNC gels, they showed a significant dependency of storage moduli on strain magnitude and exhibited a sigmoidal decrease of storage moduli G' (γ), indicating a "Payne effect" softening phenomenon.[39] Because no reduction in the storage moduli was observed in the strain−sweep measurements for covalently cross-linked hydrogels, nanocomposite hydrogels present elastic solid features at both small and large deformations, suggesting the reduction in the storage moduli in nanocomposite hydrogels was mainly attributed to reversible breakdown of the cross-linked structures. In fact, this large dependency of the storage moduli on the strain magnitude for CNC hydrogels is in agreement with the result that CNC nanocomposite hydrogels possess more efficient energy dissipation and stress relaxation process than covalently cross-linked hydrogels.

Constraint Polymer. Polymer chains are unable to cross each other and lead to the formation of topological constrains, which play a key role in the viscoelastic properties of polymers. Thus, it is attractive to know the mobility of the polymer chains around the CNC surface and demystify how the presence of CNC affects their mobility. The reversible interactions between CNC and polymer chains promote this mobility and contribute to the energy dissipative process thereby. The decrease in loss factor indicates the reduction of chain mobility, and the relative peak area is proportional to the volume of the constrained chains.[40,41] The dynamic shear measurements were performed (Figure 8a), and the results showed that a significant portion of polymer chains became constrained on the CNC surface with

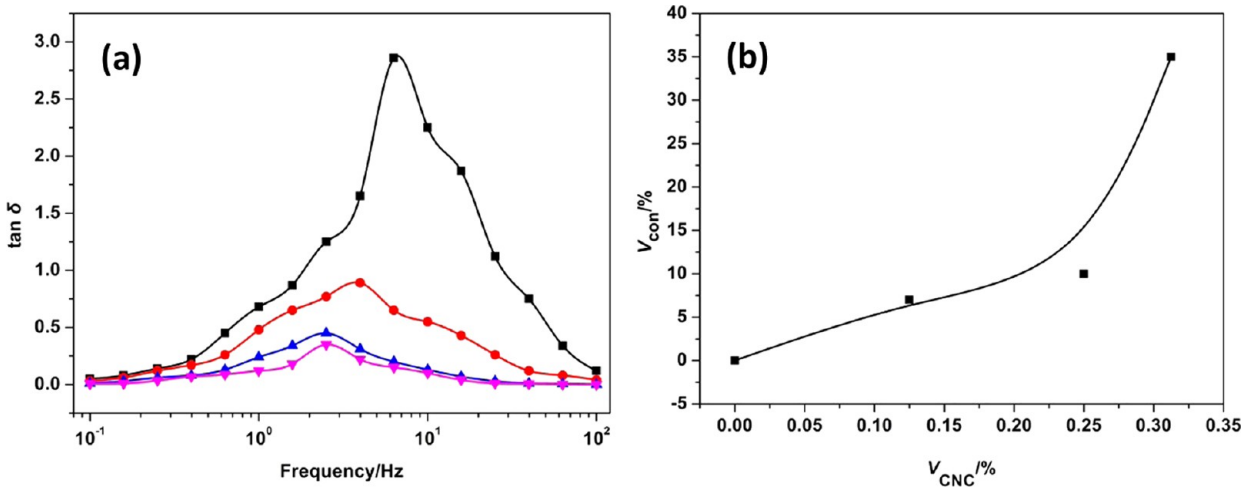

Figure 8. Constraint chains in CNC/PAA nanocomposite hydrogels. (a) Loss factor (tan δ) as a function of frequency at (■) 0 wt %, (●) 0.2 wt %, (▲)0.4 wt %, and (▼) 0.5 wt % of CNC. (b) Volume of constrained polymer chains as a function of CNC volume fraction by calculating tan δ peak in Figure 8a.

increasing of CNC fractions. The constrained chain volume and the amount of CNC can be correlated by a power law relation (Figure 8b)

$$InV_{con} = 1.78 \times InV_{CNC} + 0.21 \quad (1)$$

where V_{con} and V_{CNC} is the volume fraction of constrained polymer chains and CNC, respectively (assuming a density of CNC 1.6 g/cm^3).[7] It is shown that a low loading of CNC could constrain a huge amount of polymer chains, which intrigues us to clarify the relationship between the network structure and mechanical properties of the nanocomposite materials. During the in situ free radical polymerization, the macroradical PAA chains grow on the surface of CNC and form the core−shell structure by strong interactions. This "interaction zone" hypothesis has been advanced to rationalize the reinforcement of polymer materials and suggests that a layer near the surface of the particles exhibits significantly different dynamics from those of the bulk matrix and leads to effective increase in the modulus.[42−44] For current CNC/PAA systems, there may exist an associative equilibrium between CNC and polymer chains during the growth of clusters, where polymer chains may interact with one CNC or different CNCs. At the beginning of polymerization, primary nanoparticles "nucleate" first and then aggregate into larger secondary particles. A chain may be immobilized on a single CNC surface, whereas with an increase of the CNC concentration, the attached polymer (shell) is more likely to associate with other CNCs rather than with free polymer chains (dangling or loop chains). Then the polymer chains can wrap around neighboring CNCs and lead to the formation of interconnected CNC/PAA clusters with a size up to several hundred nanometers. The increased modulus and reduced polymer chain mobility at a high CNC concentration indicate the formation of a more rigid network. According to recent arguments on the nanoparticle reinforcement mechanism, the well-dispersed particles form a "bridge network" and act as physical cross-links,[24,25] which is in agreement with the results that the individual CNC/PAA nanoparticles become interpenetrated among neighboring clusters, leading to a stable network even in the absence of a chemical cross-linking agent.

4. DISCUSSION

In view of the dynamic nature of supermolecular architectures, the individual cluster consists of small molecules (gelators) that, in an appropriate concentration, could self-assemble into nanoscale network structures.[2,3] This process is always driven by noncovalent interactions (hydrogen bonding, van der Waals interactions, and electrostatics) into a higher order structure that consists of a spanning network.[8] In the case of CNC/PAA nanocomposites, the assembly of the gels can be easily fabricated from a solution of small molecule precursors under the proper conditions, and aggregates into a stable network. According to the classical equilibrium theory,[45] particle stability in a nanocomposite depends on several parameters, such as polymer chain−filler interaction, particle volume fraction and aspect ratio, and degree of chain polymerization, which largely determine the particle distribution through either depletion-induced phase separation or the formation of a particle bridged network.

Increases in the elastic moduli of the hydrogels are simply ascribed to the increase in the cross-linking level irrespective of the type of cross-links, whereas chemically cross-linked hydrogels lead to an increase in the elastic moduli and brittleness simultaneously due to the high cross-linking levels.[2] However, for the nanocomposite hydrogels, the high aspect ratio of CNC leads to the large interact junctions between CNC and polymer chains, which is favorable to achieve a higher elastic modulus as well as toughness (work to fracture determined by the area under the stress−strain curves). These features in mechanical properties can be interpreted by the responses of hydrogels to dynamic shear deformation at both small and large amplitudes. From Figure 7, it has been indicated that the nanocomposite hydrogels behave as an elastic solid at small deformations and exhibit viscoelastic properties at large deformations, where the accumulated energy in hydrogels can be efficiently released by this dynamic process.

The viscoelastic behaviors of nanocomposite hydrogels can be recognized from the oscillatory shear analysis. From the Maxwell model view, the nanocomposite hydrogel may be defined as a combination of elastic spring and viscous damper.[46] At low deformations, the network is seen as elastic and leads to frequency independence of storage modulus. The

part dissociation and subsequent network rearrangement of CNC/polymer clusters under stretching lead to the strong attached CNCs within a network, where viscous characteristics are expected at high deformations, especially when compared to the chemically cross-linked counterparts. Furthermore, because the dynamic network arrangement is sensitive to stress, the energy accumulated in CNC/polymer clusters can be efficiently release by this reversible process (Figure 3, Supporting Information). The above analysis of unique viscoelastic properties is consistent with the reduction of storage moduli with strain from large amplitude shear measurements. According to this model, the increase of CNC concentration would improve the level of elasticity and viscosity of hydrogels, which is validated by the larger interconnect zone and a steeper decrease in the storage moduli with increasing of strain. Additionally, the advantage of using a high aspect ratio of CNC on improving the mechanical properties is also consistent with this assumption. Increasing the interface between CNC and polymer chains promotes the elastic component and the capacity to dampen deformation stress, leading to the higher elastic moduli and formation of a larger interconnecting region. Therefore, the hydrogels loaded with the higher aspect ratio of CNC possess stronger elastic network and higher resistance against both deformation and crack propagation. Whereas for a covalently cross-linked hydrogel, it can be described as a system that possesses only an elastic spring component. Thus, a large amount of stress may accumulate on the extended network due to the absence of energy dissipative process, and storage moduli are independent of both frequency and strain magnitude. In fact, the increase of BIS concentration only increases the number of springs and the stress accumulation level even at a small strain, leading to fragility of the materials.

Before concluding this paper, the mechanism for preparation of clay/polymer nanocomposite hydrogels developed by Haraguchi et al.[23] is worth discussing in the context of the current work. According to their investigation, the monomers (*N*-isopropylacrylamide) were bound to the clay surface via nonpermanent interactions between clay and monomers. Combined with the facts that (1) the CNC surface has a high hydrophilicity, (2) cellulose is anchored with double bonds after silanization,[29] and (3) the initiator can be attached to the CNC surface via ionic interactions, the reaction starts with the generation of primary radical sites on the CNC surface and the vinyl monomer (acrylic acid) strongly anchors to the CNC surface. The flexible chains grow mainly around the surface of CNC until they terminate by recombination with other macroradicals. The propagated chains may bind to the surface of other CNCs, leading to the bridged CNCs and cross-linked network. The elastic modulus of the network is mainly determined by the CNC concentration, and the nanocomposite hydrogels exhibit an effective energy dissipation process in the whole observed CNC concentrations, suggesting the dynamic attachment/deassociation equilibrium during the stress deformation. Therefore, the interactions between CNC and polymer chains dominate the rubbery elasticity of the nanocomposite hydrogels.

5. CONCLUSIONS

The network structures and interfacial interactions have been studied using a facile nanocomposite hydrogel synthetic platform. TEM observations of hydrogels under different stretched states indicate the pore size and pore wall changes during deformation and polymer chains rearrangement on CNC surface. The tensile measurements show that the aspect ratio of CNC has a significant impact on nanocomposite hydrogel mechanical properties. The modulus enhancement of the nanocomposite hydrogels follows a power law with the volume of the constrained polymer. The large network dissociation zones in deformation with a stepwise dissociation process for nanocomposite hydrogels explains the nanocomposite hydrogel's excellent energy dissipation process and pronounced viscoelasticity, which is considered to be the underlying reason for their high toughness and flexibility. Considering the already sustainable and viable bulk process of manufacturing CNCs, further combining the responsive polymer chains to this synthetic platform would broaden the practical application of cellulose-based nanocomposite materials.

■ ASSOCIATED CONTENT

Supporting Information

Scheme of CNC−PAA network interactions, calculation of cellulose nanocrystals surface charge, constrained polymer fraction in Figure 8, TEM images of CNCs obtained from pulp fiber with different surface charges and possible network arrangement during deformation. This material is available free of charge via the Internet at http://pubs.acs.org.

■ AUTHOR INFORMATION

Corresponding Author

*J. Yang. Tel: 86-10-62338152. E-mail: yangjun11@bjfu.edu.cn.

Notes

The authors declare no competing financial interest.

■ ACKNOWLEDGMENTS

This work was financially supported by Fundamental Research Funds for the Central Universities (TD2011-10), Beijing Forestry University Young Scientist Fund (BLX2011010), and Research Fund for the Doctoral Program of Higher Education of China (20120014120006).

■ REFERENCES

(1) Pyun, J.; Matyjaszewski, K. *Chem. Mater.* **2001**, *13*, 3436−3448.
(2) Lu, Z. D.; Yin, Y. D. *Chem. Soc. Rev.* **2012**, *41*, 6874−6887.
(3) Das, D.; Kar, T.; Das, P. K. *Soft Matter* **2012**, *8*, 2348−2365.
(4) Ning, N. Y.; Fu, S. R.; Zhang, W.; Chen, F.; Wang, K.; Deng, H.; Zhang, Q.; Fu, Q. *Prog. Polym. Sci.* **2012**, *37*, 1425−1455.
(5) Miao, C.W.; Hamad, W.Y. *Cellulose* **2013**, *20*, 2221−2262.
(6) Habibi, Y.; Lucia, L. A.; Rojas, O. J. *Chem. Rev.* **2010**, *110*, 3479−3500.
(7) Moon, R. J.; Martini, A.; Nairn, J.; Simonsen, J.; Youngblood, J. *Chem. Soc. Rev.* **2011**, *40*, 3941−3994.
(8) Kumar, S.; Hofmann, M.; Steinmann, B.; Foster, E. J.; Weder, C. *ACS Appl. Mater. Interfaces* **2012**, *4*, 5399−5407.
(9) Lee, K. Y.; Tammelin, T.; Schulfter, K.; Kiiskinen, H.; Samela, J.; Bismarck, A. *ACS Appl. Mater. Interfaces* **2012**, *4*, 4078−4086.
(10) Tingaut, P.; Zimmermann, T.; Sèbe, G. *J. Mater. Chem.* **2012**, *22*, 20105−20111.
(11) Lin, N.; Huang, J.; Dufresne, A. *Nanoscale* **2012**, *4*, 3274−3294.
(12) Vermonden, T.; Censi, R.; Hennink, W. E. *Chem. Rev.* **2012**, *112*, 2853−2888.
(13) Yang, X. Y.; Zhang, G. X.; Zhang, D. Q. *J. Mater. Chem.* **2012**, *22*, 38−50.
(14) Shibayama, M. *Soft Matter* **2012**, *8*, 8030−8038.
(15) Seiffert, S.; Sprakel, J. *Chem. Soc. Rev.* **2012**, *41*, 909−930.
(16) Rose, S.; Marcellan, A.; Hourdet, D.; Creton, C.; Narita, T. *Macromolecules* **2013**, *46*, 4567−4574.

(17) Cui, J.; Lackey, M. A.; Tew, G. N.; Crosby, A. J. *Macromolecules* **2012**, *45*, 6104−6110.
(18) Fox, J.; Wie, J. J.; Greenland, B. W.; Burattini, S.; Hayes, W.; Colquhoun, H. M.; Mackay, M. E.; Rowan, S. J. *J. Am. Chem. Soc.* **2012**, *134*, 5362−5368.
(19) Rose, S.; Dizeux, A.; Narita, T.; Hourdet, D.; Marcellan, A. *Macromolecules* **2013**, *46*, 4095−4104.
(20) Haque, M. A.; Kurokawa, T.; Kamita, G.; Gong, J. P. *Macromolecules* **2011**, *44*, 8916−8924.
(21) Gong, J. P.; Katsuyama, Y.; Kurokawa, T.; Osada, Y. *Adv. Mater.* **2003**, *15*, 1155−1158.
(22) Okumura, Y.; Ito, K. *Adv. Mater.* **2001**, *13*, 485−487.
(23) Haraguchi, K.; Takehisa, T. *Adv. Mater.* **2002**, *14*, 1120−1124.
(24) Riggleman, R. A.; Toepperwein, G.; Papakonstantopoulos, G. J.; Barrat, J. L.; Pablo, J. J. *J. Chem. Phys.* **2009**, *130*, 244903.
(25) Gersappe, D. *Phys. Rev. Lett.* **2002**, *89*, 058301.
(26) Xu, X. Z.; Liu, F.; Jiang, L.; Zhu, J. Y.; Haagenson, D.; Wiesenborn, D. P. *ACS Appl. Mater. Interfaces* **2013**, *5*, 2999−3009.
(27) Rusli, R.; Shanmuganathan, K.; Rowan, S. J.; Weder, C.; Eichhorn, S. J. *Biomacromolecules* **2011**, *12*, 1363−1369.
(28) Goffin, A. L.; Raquez, J. M.; Duquesne, E.; Siqueira, G.; Habibi, Y.; Dufresne, A.; Dubois, P. *Biomacromolecules* **2011**, *12*, 2456−2465.
(29) Abdelmouleh, M.; Boufi, S.; Salah, A.; Belgacem, M. N.; Gandini, A. *Langmuir* **2002**, *18*, 3203−3208.
(30) Taipina, M. O.; Ferrarezi, M. M. F.; Yoshida, I. V. P.; Gonçalves, M. C. *Cellulose* **2013**, *20*, 217−226.
(31) Harris, J. R. *Negative Staining and Cryoelectron Microscopy: The Thin Film Techniques*; BIOS Scientific Publishers: Oxford, U.K., 1997; p 124.
(32) Harris, B. *Engineering Composite Materials*; IOM Communications Ltd.: London, 1999; p 105.
(33) Eichhorn, S. J. *Soft Matter* **2011**, *7*, 303−315.
(34) Takayanagi, M.; Minami, S.; Uemura, S. *J. Polym. Sci., Part C: Polym. Symp.* **1964**, *5*, 113−122.
(35) Favier, V.; Chanzy, H.; Cavaillé, J. Y. *Macromolecules* **1996**, *28*, 6365−6367.
(36) Roy, D.; Semsarilar, M.; Guthriea, J. T.; Perrier, Sébastien. *Chem. Soc. Rev.* **2009**, *38*, 2046−2064.
(37) Webber, R. E.; Creton, C.; Brown, H. R.; Gong, J. P. *Macromolecules* **2007**, *40*, 2919−2927.
(38) Mujtaba, A.; Keller, M.; Ilisch, S.; Radusch, H. J.; Thurn-Albrecht, T.; Saalwachter, K.; Beiner, M. *Macromolecules* **2012**, *45*, 6504−6515.
(39) Payne, A. R. *J. Appl. Polym. Sci.* **1962**, *6*, 57−63.
(40) Zhang, X. G.; Loo, L. S. *Macromolecules* **2009**, *42*, 5196−5207.
(41) Rao, Y. Q.; Pochan, J. M. *Macromolecules* **2007**, *40*, 290−296.
(42) Papakonstantopoulos, G. J.; Yoshimoto, K.; Doxastakis, M.; Nealey, P. F.; Pablo, J. *Phys. Rev. E: Stat., Nonlinear, Soft Matter Phys.* **2005**, *72*, 031801.
(43) Mackay, M. E.; Dao, T. T.; Tuteja, A.; Ho, D. L.; Horn, B. V.; Kim, H. C.; Hawker, C. J. *Nat. Mater.* **2003**, *2*, 762−766.
(44) Anderson, B. J.; Zukoski, C. F. *Macromolecules* **2009**, *42*, 8370−8384.
(45) Treloar, L. R. G. *The Physics of Rubber Elasticity*; Clarendon Press: Oxford, U.K., 2005; pp 214−218.
(46) Mark, J. E.; Erman, B. *Rubberlike Elasticity A Molecular Primer*; Cambridge University Press: Cambridge, U.K., 2007; p 210.